5-2011

A watershed-scale assessment of a process soil CO_2 production and efflux model

Diego Andrés Riveros-Iregui
University of Nebraska - Lincoln, driveros2@unl.edu

Brian L. McGlynn
Montana State University, Bozeman

Lucy A. Marshall
Montana State University, Bozeman

Daniel L. Welsch
Canaan Valley Institute, Davis, West Virginia

Ryan E. Emmanuel
Appalachian State University

See next page for additional authors

A watershed-scale assessment of a process soil CO_2 production and efflux model

Diego A. Riveros-Iregui,[1] Brian L. McGlynn,[2] Lucy A. Marshall,[2] Daniel L. Welsch,[3] Ryan E. Emanuel,[4,5] and Howard E. Epstein[6]

Received 26 August 2010; revised 18 January 2011; accepted 25 January 2011; published 28 May 2011.

[1] Growing season soil CO_2 efflux is known to vary laterally by as much as seven fold within small subalpine watersheds (<5 km^2), and such degree of variability has been strongly related to the landscape-imposed redistribution of soil water. Current empirical or process models offer low potential to simulate this variability or to simulate watershed-scale dynamics of soil CO_2 efflux. We modified an existing process soil CO_2 production and efflux model to include spatially variable soil moisture, and applied it to a well-studied and moderately complex watershed of the northern Rocky Mountains. We started at the point scale and progressively modeled processes up to the watershed scale. We corroborated model performance using an independent data set of soil CO_2 efflux measurements from 53 sites distributed across the 393 ha watershed. Our approach (1) simulated the seasonality of soil CO_2 efflux at riparian sites; (2) reproduced short-term (diel) dynamics of soil CO_2 concentration ($[CO_2]$) at riparian sites, particularly observed hysteresis patterns in the soil $[CO_2]$–soil temperature relationship; and (3) simulated growing season estimates of soil CO_2 efflux at dry sites across the landscape (98% of area). Model limitations included poor simulation of growing season (cumulative) soil CO_2 efflux at sites with a large drainage area, likely as a result of poorly modeled soil water content and challenges in parametrization of root and microbial activities. Our study provides important insight into coupling hydrological and biogeochemical models at landscape scales, and highlights the role of landscape structure and heterogeneity when modeling spatial variability of biogeochemical processes.

Citation: Riveros-Iregui, D. A., B. L. McGlynn, L. A. Marshall, D. L. Welsch, R. E. Emanuel, and H. E. Epstein (2011), A watershed-scale assessment of a process soil CO_2 production and efflux model, *Water Resour. Res., 47*, W00J04, doi:10.1029/2010WR009941.

1. Introduction

[2] Growing season soil CO_2 efflux is known to vary laterally by as much as seven fold within small subalpine watersheds (<5 km^2), and such degree of variability has been strongly related to the landscape-imposed redistribution of soil water [*Riveros-Iregui and McGlynn*, 2009]. Empirical models of soil CO_2 efflux abound based on derived relationships with soil temperature [e.g., *Kucera and Kirkham*, 1971; *Ratkowsky et al.*, 1982; *Winkler et al.*, 1996], soil water content [e.g., *Orchard and Cook*, 1983; *Davidson et al.*, 2000; *Liu et al.*, 2002; *Yuste et al.*, 2003], substrate [e.g., *Raich and Nadelhoffer*, 1989; *Ryan et al.*, 1996; *Janssens et al.*, 2001; *Reichstein et al.*, 2003], or morphologic variables such as upslope accumulated area (UAA) [*Riveros-Iregui and McGlynn*, 2009] and microtopography [*Lee et al.*, 2011]. On the other hand, process models represent the mechanisms known to govern soil CO_2 efflux, and are derived from system examination and physical evidence [e.g., *Parton et al.*, 1987; *Rastetter et al.*, 1991; *Potter et al.*, 1993; *Suarez and Simunek*, 1993; *Rastetter et al.*, 1997; *Fang and Moncrieff*, 1999; *Welsch and Hornberger*, 2004]. However, both empirical and process models to date offer low potential to simulate the observed, natural variability of soil CO_2 efflux across mountainous catchments.

[3] A common problem in current soil CO_2 efflux models, and in many catchment-scale biogeochemical models, is the omission of spatial and temporal variability of soil moisture. It has been recently demonstrated that soil water content can control the spatial [*Pacific et al.*, 2008; *Riveros-Iregui and McGlynn*, 2009] and temporal [*Riveros-Iregui et al.*, 2007; *Riveros-Iregui et al.*, 2008; *Pacific et al.*, 2009] variability of soil CO_2 efflux in subalpine systems of the western United States or in boreal forest systems of Alaska [*Kane et al.*, 2006]. To date, a robust implementation of the lateral distribution of soil water into biogeochemical models is lacking. Understanding the effects of soil moisture heterogeneity on soil CO_2 efflux from diel to seasonal scales, and from the point to the ecosystem scale, will enhance process knowledge of the spatial variability of biogeochemical processes across many ecosystems.

[1]School of Natural Resources, University of Nebraska, Lincoln, Nebraska, USA.
[2]Department of Land Resources and Environmental Sciences, Montana State University, Bozeman, Montana, USA.
[3]Canaan Valley Institute, Davis, West Virginia, USA.
[4]Department of Geology, Appalachian State University, Boone, North Carolina, USA.
[5]Now at Department of Forestry and Environmental Resources, North Carolina State University, Raleigh, North Carolina, USA.
[6]Department of Environmental Sciences, University of Virginia, Charlottesville, Virginia, USA.

0043-1397/11/2010WR009941

[4] We applied an existing process soil CO_2 production model [*Fang and Moncrieff*, 1999; *Welsch and Hornberger*, 2004] in combination with a recently developed CO_2 production and diffusion model [*Riveros-Iregui et al.*, 2007], to a well-studied subalpine watershed of the northern Rocky Mountains. We implemented this model by progressively adding process understanding starting at the point scale and advancing to the watershed scale. Given our catchment-scale focus, we used a single-layer model because it is useful to examine the effects of laterally variable environmental gradients (e.g., soil moisture) on catchment scale biogeochemistry. We acknowledge that a multilayer model may yield different (and certainly more detailed) results across individual soil profiles. However, we were encouraged by the pragmatic approach of *Raupach and Finnigan* [1988], who highlight the usefulness of single-layer models in systems with a length scale much larger than that of the multilayered processes themselves (e.g., medium- or large-scale catchments). Our study takes advantage of a well-established and efficient hydrologic model that simulates the lateral variability of soil water content across the landscape, as well as the convergence and divergence of unsaturated flow. In this paper we seek (1) to critically assess the performance of a soil CO_2 process and efflux model applied across a moderately complex catchment; (2) to investigate the role of spatial and temporal variability of soil moisture on simulated soil CO_2 efflux; and (3) to corroborate model performance using an independent data set of CO_2 efflux measurements at distributed sites across the same watershed. We address two outstanding research questions: the role of hydrology as a spatial and temporal control of soil CO_2 efflux, and the role of model-data comparison in the development of biogeochemical models in mountainous watersheds.

2. Study Site

[5] The study site was the Tenderfoot Creek Experimental Forest (TCEF), a subalpine catchment located in the Little Belt Mountains of central Montana. This forest is representative of the subalpine ecosystems of the northern Rocky Mountains and is subject to a steady seasonal drydown in soil moisture [*Woods et al.*, 2006; *Riveros-Iregui et al.*, 2007]. The 393 ha catchment of interest contains a second-order perennial stream, Stringer Creek that drains into Tenderfoot Creek, which ultimately drains into the Missouri River. At the TCEF, freezing temperatures and snow can occur any month of the year, and the mean annual temperature is 0°C [*Farnes et al.*, 1995]. During the period of this study (21 June 21–2 September 2006), air temperature ranged from 28.8°C (30 July) to −2.1°C (2 September), with an average of 13.6°C. The growing season for the majority of the TCEF can extend from 45 to 90 days, decreasing in length toward the ridges. Cumulative precipitation during the period of this study was 42 mm with the highest daily precipitation falling on 29 June (9.2 mm), and monthly precipitation of 9.8 mm (21–30 June), 23.4 mm (July), and 8.9 mm (August). Mean annual precipitation is 880 mm with a majority (>70%) falling as snow [*Farnes et al.*, 1995]. The Stringer Creek watershed ranges in elevation from 2090 to 2421 m and has a full range of slope, aspect, and topographic convergence and divergence. Because this catchment has been the focus of several hydrologic and biogeochemical studies in the last few years [*Riveros-Iregui et al.*, 2007; *Pacific et al.*, 2008; *Riveros-Iregui*, 2008; *Riveros-Iregui et al.*, 2008; *Jencso et al.*, 2009], Stringer Creek watershed is an ideal site to assess the performance of a coupled hydrological-biogeochemical model at the landscape scale.

[6] The two predominant ecosystems at Stringer Creek are riparian meadows (near the Stringer Creek channel) and upland forests. Vegetation cover at riparian meadows is dominated by *Calamagrostis canadensis* (bluejoint reedgrass), whereas vegetation in upland forests is dominated by *Pinus contorta* (lodgepole pine) and to a lesser extent *Abies lasiocarpa* (subalpine fir) and *Picea Engelmannii* (Engelmann spruce). *Vaccinium scoparium* (whortleberry) is the predominant understory species. Given its relatively simple and homogenous vegetation cover, Stringer Creek is a suitable site to implement a model focused on effects of soil water content on soil CO_2 efflux at the watershed scale.

3. Model

3.1. Soil Water Content Model

[7] Recent studies in subalpine ecosystems have highlighted the importance of the lateral redistribution of soil water as a control of soil CO_2 production and efflux, both temporally [*Riveros-Iregui et al.*, 2007] and spatially [*Riveros-Iregui and McGlynn*, 2009]. To model soil water content at the catchment scale, we applied TOPMODEL [*Beven and Kirkby*, 1979] for its ability to describe flow and connectivity within a catchment on the basis of topographic similarity among grid cells of a digital elevation model. We employed a version of TOPMODEL modified by *Scanlon et al.* [2005] that estimates shallow, unsaturated flow (i.e., lateral soil water flux q_l) in addition to saturated, groundwater flow and overland flow for each grid cell. This version of TOPMODEL also included a calibrated parameter to estimate groundwater recharge (i.e., vertical soil water flux q_v), and a mechanistic model of vertical flow through the soil-plant-atmosphere continuum [*Emanuel et al.*, 2010] to develop a soil water balance for each grid cell (5 m) of the watershed,

$$\frac{d\theta}{dt} = \frac{1}{z_r}(I - ET - q_v - q_l), \tag{1}$$

where θ is volumetric soil moisture, q_v is vertical soil water flux, q_l is lateral soil water flux, z_r is the depth of the root zone, I is infiltration, and ET is evapotranspiration (See Table 1). Infiltration and ET were modeled from lidar-derived vegetation characteristics within each grid cell and prescribed meteorological conditions interpolated from seven meteorological stations within the watershed following *Jolly et al.* [2005] and *Emanuel et al.* [2010]. Because topography, vegetation, and meteorological conditions vary across the watershed, the soil water balance (2-D; vertical and along the hillslope) was solved separately for each grid cell of the watershed for each half-hour of the 2006 growing season (21 June through 2 September 2006). The model was recently applied to the Stringer Creek watershed, demonstrating its ability to simulate water-controlling processes at the catchment scale [*Emanuel et al.*, 2010]. Model output was compared to runoff measured by the US Forest Service

at the catchment outlet and to total ET measured by an eddy covariance tower [*Emanuel et al.*, 2010], validating the use of the model to accurately simulate seasonal hydrologic balance of Stringer Creek catchment. Despite differences in absolute magnitude in particular toward the dry end of the soil water content range (see auxiliary material), seasonal trends of simulated soil water content replicated our observations very closely ($r^2 = 0.97$).

[8] Soil CO_2 production is typically calculated as a function of water stress on plant and microbial activities [*Simunek and Suarez*, 1993; *Welsch and Hornberger*, 2004]; thus we calculated soil water matric potential or soil tension (h) as a surrogate for water stress by solving a widely applied soil moisture–soil tension relationship [*van Genuchten*, 1980]

$$h = \frac{\left\{\left[\frac{(\theta_S - \theta_r)}{(\theta - \theta_r)}\right]^{\frac{1}{m}} - 1\right\}^{\frac{1}{n}}}{\alpha}, \quad (2)$$

where θ_s is the saturated water content, θ_r is the residual water content, α is a fitting parameter for tension at air entry, m is given by $m = 1 - (1/n)$, and n is a fitting parameter estimated from observed data. The van Genuchten relationship has been widely applied and deemed accurate when simulating diffusion as a function of air−filled porosity across multiple soil types and porosities [*Moldrup et al.*, 2005a, 2005b].

3.2. Soil Temperature Model

[9] Soil temperature controls soil CO_2 production and efflux at short- and long-time scales [e.g., *Lloyd and Taylor*, 1994; *Winkler et al.*, 1996]. To model soil temperature for the entire catchment, we used interpolated, distributed air temperature at 10 m grid resolution derived from the Spatial Observation Gridding System (SOGS) [*Jolly et al.*, 2005] for the period between 21 June and 2 September 2006, at half-hour intervals. This scale-independent system is known to yield a mean absolute error smaller than 2°C [*Jolly et al.*, 2005]. We then used the approximation of *Kang et al.* [2000] (developed to simulate spatiotemporal variability of soil temperature in forested soils) to calculate soil temperature at half-hour intervals. This relationship assumes that soil temperature can be estimated at any depth (z) as follows: when $A_j > T_{S-j-1}$,

$$T_{S-j}(z) = T_{S-j-1}(z) + \left[A_j - T_{S-j-1}(z)\right] \exp\left[-z\left(\frac{\pi}{k_s p}\right)^{\frac{1}{2}}\right] \exp[-k(LAI + \text{litter})] \quad (3)$$

and when $A_j \leq T_{S-j-1}$,

$$T_{S-j}(z) = T_{S-j-1}(z) + \left[A_j - T_{S-j-1}(z)\right] \exp\left[-z\left(\frac{\pi}{k_s p}\right)^{\frac{1}{2}}\right] \exp(-k \times \text{litter}), \quad (4)$$

where A_j is air temperature at the time j, T_S is soil temperature, k_s is the soil thermal diffusivity (1.54×10^{-3} cm^2/s), p is the period of diurnal temperature variation (86,400 s), and k is the extinction coefficient from the Beer-Lambert Law for radiation through canopy as a function of leaf area index (*LAI*) and ground litter *LAI* equivalent. Measured *LAI* in the forest (98% of watershed area) ranged from 1.1 to 1.35, whereas measured *LAI* in riparian areas (2% of watershed area) ranged from 0.8 or less at the beginning of the season, to a high of 2.0 in the middle of the growing season, rapidly decreasing by late summer with grass senescence (unpublished data). Thus for simplicity in the soil temperature model, we used a *LAI* value of 1.2 m^2 m^{-2} for both vegetation covers, as well as ground litter value of 1.5 m^2 m^{-2}, throughout the growing season. While we acknowledge potential inaccuracies introduced by this assumption especially in riparian areas, such inaccuracies were typically small (~0.8°C error in T_S for every change of 0.5 m^2 m^{-2} in *LAI* at $T_S = 18$°C, and smaller at lower temperatures) and the model was a good predictor of the seasonality of soil temperature. Based on calibration with measured soil temperature at two sites, the estimated mean absolute error for

Table 1. Variables Included in Models of Soil Water Content, Soil Temperature, and Soil CO_2 Production and Efflux, as well as in the Terrain Aanalysis

Variable	Description	Dimensions
	Soil Water Content	
z_r	Depth to root zone	m
I	Infiltration	m s^{-1}
ET	Evapotranspiration	m s^{-1}
q_v	Vertical water flux	m s^{-1}
q_l	Lateral water flux	m s^{-1}
α	Fitting parameter for tension at air entry	
m	Fitting parameter	
n	Fitting parameter	
h	Soil tension	m
θ	Soil water content	m^3 m^{-3}
θr	Residual soil water content	m^3 m^{-3}
θs	Saturated soil water content	m^3 m^{-3}
	Soil Temperature	
A	Air temperature	°C
T_S	Soil temperature	°C
K_S	Soil thermal diffusivity	m^2 s^{-1}
Z	Soil depth	m
p	Period of diurnal temperature variation	s
k	Extinction coefficient	
LAI	Leaf area index	m^2 m^{-2}
	Soil CO_2 Production and Efflux	
f_a	Air-filled porosity	m^3 m^{-3}
D	Diffusion coefficient	m^2 s^{-1}
γ_A	Autotrophic respiration rate per unit biomass	g CO_2 m^{-2} s^{-1}
γ_H	Heterotrophic respiration rate per unit biomass	g CO_2 m^{-2} s^{-1}
PAR	Photosynthetically active radiation	mmol m^{-2} s^{-1}
B	Root fraction	kg m^{-3}
M	Soil organic content	kg m^{-3}
h_a	Soil tension when CO_2 production stops, soil too wet	m
h_b	Soil tension when CO_2 production is optimal	m
h_c	Soil tension when CO_2 production stops, soil too dry	m
	Landscape Analysis	
UAA	Upslope accumulated area	m^2

[1] Auxiliary materials are available in the HTML. doi:10.1029/2010WR009941.

soil temperature was lower than 1.5°C across the 74 days of the simulation and across a seasonal range of ~20°C (see auxiliary material).

3.3. Soil CO_2 Production and Efflux Model

[10] The dynamics of CO_2 in soil air can be explained by the following mass balance equation [*Riveros-Iregui et al.*, 2007]:

$$f_a \frac{\partial [CO_2]}{\partial t} = -\frac{\partial}{\partial z}\left[D(f_a)\frac{\partial [CO_2]}{\partial z}\right] + \gamma_A(B, PAR, \theta) + \gamma_H(M, T_S, \theta), \quad (5)$$

where f_a is the air-filled porosity, D is the diffusion coefficient of CO_2 in the air-filled pore space, γ_A and γ_H are the rates of CO_2 production from autotrophic and heterotrophic activities, respectively, B is root biomass, PAR is photosynthetically active radiation, and M is soil organic matter. It is important to note that PAR and T_S vary in time on a diel basis, whereas θ varies in time on a seasonal basis. As a result, there is asynchronism in the timing and effect of each variable on the resulting soil CO_2 concentration ($[CO_2]$). While equation (5) presents the dynamics of $[CO_2]$ at any given depth z, the right-hand side of equation (5) is divided into two components: a "production" component $(\gamma_A + \gamma_H)$ and a "diffusion" component $(D\frac{\partial [CO_2]}{\partial z})$. To implement the production component, we adapted the soil CO_2 production component of a previously developed model [*Fang and Moncrieff*, 1999; *Welsch and Hornberger*, 2004], and in it, B and M were based on field observations [*Riveros-Iregui and McGlynn*, 2009] and kept constant across the catchment ($B = 7.6$ kg m^{-3} and $M = 16.5$ kg C m^{-3}). PAR was scaled between 0 and 1 across the season. The model has been used across different forested ecosystems [*Moncrieff and Fang*, 1999; *Welsch and Hornberger*, 2004; *Saiz et al.*, 2007] because it includes the main effects of environmental factors (i.e., soil temperature, soil moisture, soil $[O_2]$) on the generation of soil CO_2 from plant and microbial activities. Rates of autotrophic and heterotrophic activities were calibrated based on optimal rates for θ and T_S found in the literature [*Fang and Moncrieff*, 1999; *Hamman et al.*, 2008] and corroborated with soil CO_2 efflux rates at the site [*Riveros-Iregui and McGlynn*, 2009].

[11] As presented in equation (5), production and diffusion components have opposite signs, so the diffusion component provides diffusion-limited feedback to the model at low values of f_a [see *Riveros-Iregui et al.*, 2007]. Specifically, variability in θ controls the transition from a diffusion-limited system to a production-limited system [*Riveros-Iregui et al.*, 2007]. Once CO_2 production was modeled we added the diffusion component of equation (5) to modeled production. We assumed a homogenous diffusion coefficient (D) across the watershed, based on several calculated values of D as a function of total porosity (Φ) and f_a, and using the model proposed by *Moldrup et al.* [1999]:

$$\frac{D}{D_0} = \Phi^2\left(\frac{f_a}{\Phi}\right)^{2+\frac{3}{b}}, \quad (6)$$

where D_0 is the gas diffusion coefficient in free air, b is the *Campbell* [1974] pore size distribution parameter, Φ is total soil porosity, and f_a is calculated as Φ minus θ. The b parameter was derived from the following relationship with clay fraction content (CF) ($r^2 = 0.96$) [*Clapp and Hornberger*, 1978; *Olesen et al.*, 1996; *Rolston and Moldrup*, 2002]:

$$b = 13.6CF + 3.5. \quad (7)$$

[12] This method is widely applied and it has been amply tested to model D across a range of soil types and water contents [*Baldocchi et al.*, 2006; *Kawamoto et al.*, 2006; *Resurreccion et al.*, 2007]. Solubility of CO_2 in the gas phase as well as the vertical advection by soil water were assumed negligible, given that CO_2 diffusion in the gas phase is several orders of magnitude higher than in the liquid phase [*Simunek and Suarez*, 1993; *Welsch and Hornberger*, 2004].

[13] We estimated the effects of soil tension in controlling rates of autotrophic and heterotrophic respiration (γ_A and γ_H; equation (5)). According to *Simunek and Suarez* [1993] and *Welsch and Hornberger* [2004], the CO_2 reduction coefficient $f_s(h)$ is a function of soil tension as illustrated by the following relationships:

$$f_s(h) = \frac{\log|h| - \log|h_a|}{\log|h_b| - \log|h_a|},\ h \in (h_b, h_a), \quad (8)$$

$$f_s(h) = \frac{\log|h| - \log|h_c|}{\log|h_b| - \log|h_c|},\ h \in (h_c, h_b), \quad (9)$$

$$f_s(h) = 0,\ h \in (-\infty, h_c) \cup (h_a, -\infty), \quad (10)$$

where h_b is the tension when CO_2 production is optimal, and h_a and h_c are soil tension values when respiration ceases because conditions are too wet or too dry, respectively.

3.4. Field Observations and Landscape Analysis

[14] At one riparian meadow site and one upland forest site (Figure 1), we measured volumetric soil water content (CSI model 616, Campbell Scientific Inc., Logan, UT) and soil temperature (CSI model 107, Campbell Scientific Inc., Logan, UT) 20 cm below the soil surface. At the same two sites, continuous measurements of soil $[CO_2]$ were collected with solid-state CO_2 probes (GMP221 with transmitter, Vaisala, Helsinki, Finland) installed 20 cm below the soil surface on 7 June 2006. All data were logged at 20 min intervals with a data logger (model CR10x, Campbell Scientific Inc., Logan, UT). Further details on field measurements have been described in a field-based study [*Riveros-Iregui et al.*, 2008].

[15] To validate modeled soil CO_2 efflux, we used independent measurements at 53 sites distributed across the watershed (Figure 1) collected during the 2006 growing season and reported in a previous study [*Riveros-Iregui and McGlynn*, 2009]. Although the previous study reported measurements from 62 sites, an incongruity in boundaries between the lidar-derived digital elevation imagery and actual watershed area resulted in nine fewer sites for this study. Measurements of soil CO_2 efflux were made according to procedures described by *Pacific et al.* [2008] and *Riveros-Iregui et al.* [2008]. Measurements were collected

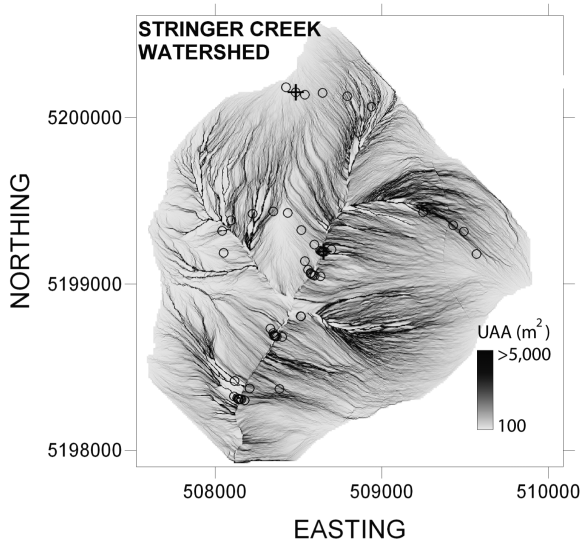

Figure 1. Location of riparian and upland calibration sites (crosses) and 53 independent measurement (validation) sites (circles). Shading represents the calculated 3 m upslope accumulated area (UAA), a metric for relative wetness potential among sites of the same watershed. See section 3 for additional details.

in triplicate every 2–7 days, using a soil respiration chamber model SRC-1 (PP Systems, Massachusetts, USA) equipped with an infrared gas analyzer (IRGA; EGM-4, PP Systems, Massachusetts, USA).

[16] To estimate relative wetness potential at each site, we calculated upslope accumulated area (UAA (m^2)) for each 3 m pixel of a digital elevation model (DEM) of the watershed (Figure 1), based on the triangular multiple flow direction algorithm [*Seibert and McGlynn*, 2007]. UAA represents the amount of area draining to a specific location in the landscape [*Beven and Kirkby*, 1979; *McGlynn and Seibert*, 2003] and serves as a metric for patterns of water flow and comparison among sites of the same watershed [*Western and Grayson*, 1998; *Grayson and Western*, 2001].

3.5. Modeling Approach

[17] The modeling approach can be divided into three steps. First, soil CO_2 production (or $[\gamma_A + \gamma_H]$ in equation (5)) was modeled at 30 min intervals at 20 cm depth for the riparian and upland sites (Figure 1). Model calibration was performed using these two sites given the good temporal coverage of observations of soil water content, soil temperature, and soil [CO_2] [*Riveros-Iregui et al.*, 2008], and using Monte Carlo analysis. This analysis has been used in parametrization of hydrological models [*Freer et al.*, 1996; *Campbell et al.*, 1999] and more recently in parametrization of ecosystem respiration models [*Knohl et al.*, 2008; *Ricciuto et al.*, 2008]. Six parameters, γ_A, γ_H, h_a, h_b, h_c, and n, were sampled randomly from uniform distributions based on the range of known variability of these parameters found in the literature [*Fang and Moncrieff*, 1999]. The process was repeated 25,000 times and in each step the parameters were used to estimate the Nash-Sutcliffe coefficient [*Nash and Sutcliffe*, 1970] of model efficiency (E). Selected values were chosen based on the set of parameters that yielded the highest E.

[18] Second, once E did not improve any further, we applied the diffusion term of equation (5), or $D\frac{\partial[CO_2]}{\partial z}$, to modeled soil CO_2 production. In doing so, we assumed only one soil layer and modeled diffusion (efflux) from a 20 cm depth to the soil surface ($z = 0$ cm), where [CO_2] was set constant at 450 ppm. Previous studies have used similar assumptions at the soil surface [*Tang et al.*, 2005; *Riveros-Iregui et al.*, 2008] and demonstrated that these assumed values do not compromise calculation of soil CO_2 efflux, as the diel variability of [CO_2] at depth is much greater than the diel variability of [CO_2] above the soil surface given the atmospheric buffer (see *Riveros-Iregui et al.* [2008] for a sensitivity analysis of this assumption). Applied this way (step 1, step 2), we used our modeling approach to test sites of the landscape that were production limited (i.e., where autotrophic and heterotrophic respirations were limited by low soil moisture) and sites of the landscape that were diffusion limited (i.e., where soil CO_2 diffusion and efflux was limited by high soil moisture). This approach also allowed us to investigate whether diffusion (modified entirely by the spatiotemporal variability of θ) played a larger role in some landscape areas than others. To date, the fundamental balance between production and diffusion has not been simultaneously implemented into soil respiration models, yet the diffusion-limited feedback emerging during high moisture can be significant in wet soils during some times of the year [*Riveros-Iregui et al.*, 2007; *Pacific et al.*, 2008, 2009].

[19] Third, once the model was parametrized and calibrated to simulate production and diffusion at the riparian meadow and upland forest sites, we applied it to the entire watershed via a 10 m digital elevation model (DEM). Results were validated using independent measurements of soil CO_2 efflux (or the resulting $D\frac{\partial[CO_2]}{\partial z}$ at the soil surface) at 53 sites distributed across the watershed [*Riveros-Iregui and McGlynn*, 2009]. We assumed a homogenous soil type (sandy loam) and depth across the entire watershed. Model performance was evaluated based on the mean absolute error (MAE) of observed and modeled efflux across the 53 sites.

4. Results

4.1. Model Parametrization

[20] The selected set of parameters based on the Monte Carlo analysis is shown in Figure 2. Each sampled model parameter is plotted against the Nash-Sutcliffe coefficient of model efficiency. This plot shows the sensitivity of individual model parameters where a strong change in the model efficiency is observed over some range of the parameter [*Freer et al.*, 1996]. Based on these plots we selected optimal values of γ_A, γ_H, h_a, h_b, h_c, and n parameters for the model (Table 2). These parameters yielded a combined Nash-Sutcliffe coefficient of model efficiency (E) of 0.0881 at the riparian site and −4.71 at the upland site. In selecting these parameters, we assumed they were constant throughout the watershed.

4.2. Long-Term (Seasonal) Dynamics

[21] The seasonal dynamics of soil [CO_2] are presented in Figure 3. At the riparian site, observed soil [CO_2] varied

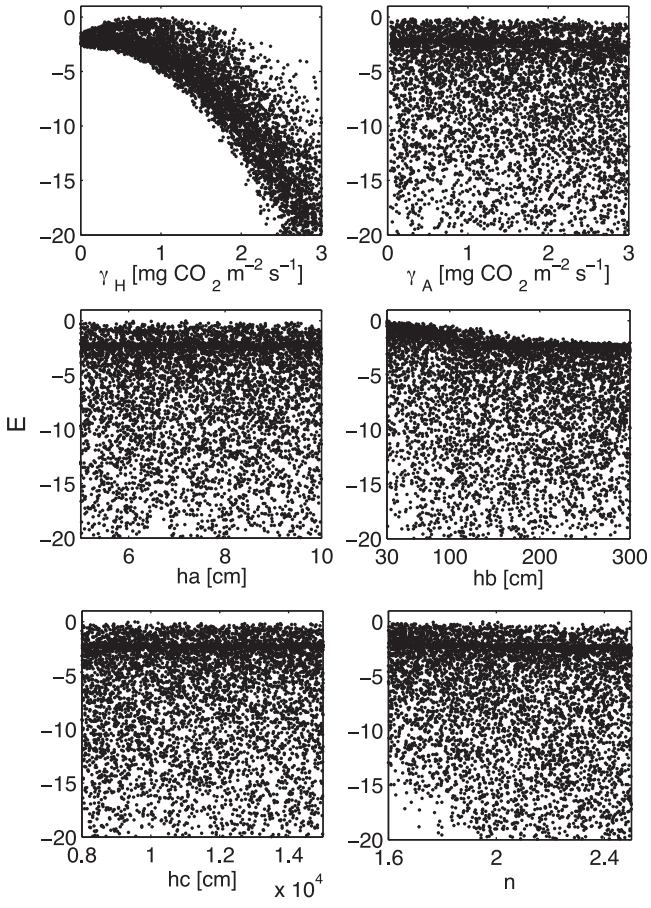

Figure 2. Monte Carlo analysis for parameter selection using the Nash-Sutcliffe coefficient of model efficiency (E). Parameters were sampled randomly from uniform distributions based on the range of variability of these parameters found in the literature. This figure demonstrates that the model was more sensitive to some parameters (e.g., heterotrophic respiration rate [γ_H]) than others (e.g., soil tension when CO_2 production stops [h_a, h_c]), and this sensitivity is asymmetric (e.g., γ_H, h_b) depending on whether the variable is increasing or decreasing.

from over 12,000 ppm at the beginning of the growing season to about 2000 ppm by the end of the summer (Figure 3). Applying only the production component of the model (i.e., not accounting for diffusion), modeled soil [CO_2] varied from around 5000 ppm at the beginning of the growing season to about 2000 ppm by the end of the summer, and the estimated E was 0.0881 (Figure 3a). Note that during high soil moisture periods the model did not simulate soil [CO_2] well, likely as a result of soil water content values greater than 0.25 m^3 m^{-3} and associated limitation in gas diffusion. When accounting for diffusion, soil [CO_2] were better predicted and the estimated E improved from 0.0881 to 0.708 at the riparian site (Figure 3b). Similar analysis at the upland site demonstrated that E did not improve after accounting for diffusion at this site (Figure 4), likely because of much lower soil water content at this site (average $\sim$0.13 m^3 m^{-3}).

Table 2. Selected Soil CO_2 Production Model Parameters Based on Monte Carlo Analysis[a]

Parameter	Value	Range (min: max)
γ_H	0.8388	(0.23: 1.64)
γ_A	0.3283	(0.04: 2.96)
h_a	9.1137	(5.01: 9.94)
h_b	30.2073	(30.1: 134.4)
h_c	9536.3	(8005: 14,971)
n	1.743	(1.60: 2.49)

[a]Parameter range corresponds to range for the top 5% values of E.

4.3. Short-Term (Diel) Dynamics

[22] The magnitude of the short-term (diel) variability in soil [CO_2] was well simulated by the model at the riparian site, suggesting appropriate parametrization and incorporation of soil temperature and *PAR* into model structure. Observed diel range in soil [CO_2] varied from $\sim$5000 ppm on 13 June, to 2000 ppm on 23 June, to near zero by the end of July (Figure 5). An additional strength of the model was its ability to simulate observed hysteresis in the soil [CO_2]–soil temperature relationships throughout the growing season (Figures 5 and 6). The diel range of soil [CO_2] was not simulated as well at the upland site. While the diel range of observed soil [CO_2] was low (little or no hysteresis; Figure 6), modeled [CO_2] exaggerated hysteresis (i.e., the model overpredicted $\frac{\partial[CO_2]}{\partial t}$) at the dry site. Given that continuous measurements were made only at two sites with contrasting soil moisture, this feature of the model could not be further explored at other sites (e.g., intermediate sites).

4.4. Spatial Variability of Modeled Efflux

[23] Across the entire catchment, modeled soil CO_2 efflux varied from 4.6 to 26.4 mol CO_2 m^{-2} over 71 days, with a mean efflux of 11.1 mol CO_2 m^{-2} over the same period. Compared against the 53 sites, the model performed better at those locations with small drainage area (Figure 7), where despite a modest overprediction the model simulated the magnitude of seasonal fluxes well. At sites with large drainage area, however, model performance progressively declined and modeled CO_2 fluxes were increasingly underestimated (Figure 8). Lateral differences in CO_2 production and CO_2 diffusion resulted in different spatial patterns of soil CO_2 efflux at different times of the year. For example, early in the growing season (24 June) efflux range across the catchment was low (less than 2 μmol CO_2 m^{-2} s^{-1}; Figure 9). By the peak of the growing season (23 July), the range across the catchment was the largest ($\sim$8 μmol CO_2 m^{-2} s^{-1}), whereas by late August the range of catchment efflux decreased although the spatial differences remained more pronounced than during early summer.

5. Discussion

[24] The seasonality of soil [CO_2] was well simulated at the riparian site (Figure 3), especially when accounting for soil CO_2 diffusion. Despite the low soil [CO_2] after 30 July (Figure 3b), E improved from to 0.0881 to 0.701, and MAE decreased from 1690 to 1130 ppm. This is an important improvement considering [CO_2] at this site can reach over 15,000 ppm, and diffusion-limited feedback during high moisture may be significant, especially at short (e.g., diel)

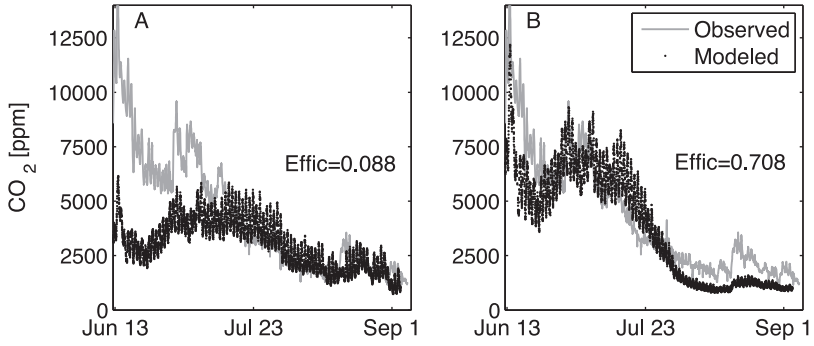

Figure 3. Seasonal soil [CO_2] at 20 cm of the riparian site applying (a) only the soil CO_2 production component of the model; and (b) the production and efflux components of the model. Model ability to simulate soil [CO_2] considerably increased when efflux component (diffusion limitation feedback) was introduced into the model.

time scales [*Riveros-Iregui et al.*, 2007; *Pacific et al.*, 2008, 2011]. At the upland site *E* did not improve after accounting for diffusion, perhaps because of significantly lower soil moisture relative to the riparian site. In fact, *E* decreased and MAE increased, suggesting that in dry soils diffusion does not limit soil CO_2 efflux (i.e., all CO_2 that is produced leaves as efflux). An issue that emerged when accounting for diffusion at low soil water content values (i.e., after 30 July in Figure 3b; or Figure 4b) was the decrease in model performance. This decrease is an artifact caused by the application of cost functions (such as *E*, MAE) across the full range of soil [CO_2]. These cost functions are more sensitive to large discrepancies, because minimizing a large error has a larger impact on MAE and *E* than minimizing a small error. It has been established that both "wet" and "dry" catchment behavior cannot always be accurately represented with a single set of parameters [*Wagener*, 2003]; thus, our findings suggest that when applying biogeochemical models at the watershed scale, caution should be taken and model parametrization and assessment should reflect, at least to a first degree, the lateral variability of soil water (wet versus dry sites) as well as its seasonality (wet versus dry times of the year).

[25] Implementing a *PAR*-dependent variable (equation (5)) as a temporal control on autotrophic activity improved the simulation of hysteresis patterns in the soil [CO_2]–soil temperature relationship at the riparian site (Figure 5). As recently demonstrated, there is a temperature independent component in soil [CO_2] that can be explained by the variability of *PAR* [*Liu et al.*, 2006; *Riveros-Iregui et al.*, 2007; *Vargas and Allen*, 2008]. However, similar analysis at the upland site showed that the model overestimated hysteresis at this site (e.g., 23 July; Figure 6), likely because the effects of *PAR* on soil CO_2 efflux are different between sites. This suggests that the parametrization of *PAR* on soil CO_2 efflux at the catchment scale is useful but it needs to be further explored in combination with variable vegetation cover and dynamic soil moisture conditions.

[26] The model simulated cumulative rates of efflux at those areas with low UAA better than at areas with high UAA. In fact, MAE was 6.6 mol CO_2 m^{-2} for 71 days across the 53 sites, but it was only 1.75 mol CO_2 m^{-2} for the same period at those sites with UAA below $\sim$1600 m^2 (32 sites total; Figure 7). At sites with large UAA, the model did not perform well because of poorly modeled soil water content. Similar deficiencies had been observed while using the model across gradients of soil moisture in other ecosystems [*Moncrieff and Fang*, 1999; *Welsch and Hornberger*, 2004; *Saiz et al.*, 2007]. Because modeling the spatially variability of soil water content remains an ample area of research, it is anticipated that improving catchment scale biogeochemical models will remain dependent upon uncertainties of models of soil water content. A second deficiency in our modeling approach lies in our understanding of catchment scale microbial processes and in the observed sensitivity of the model to microbial respiration rates. Figure 2 demonstrates that the model appears

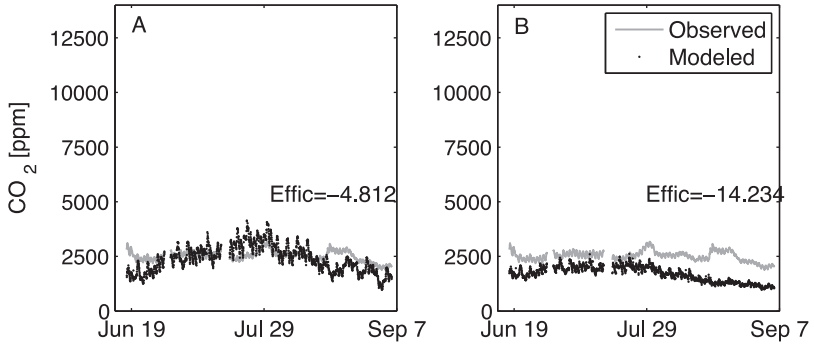

Figure 4. Seasonal soil [CO_2] at 20 cm of the upland site applying (a) only the soil CO_2 production component of the model; and (b) the production and efflux components of the model.

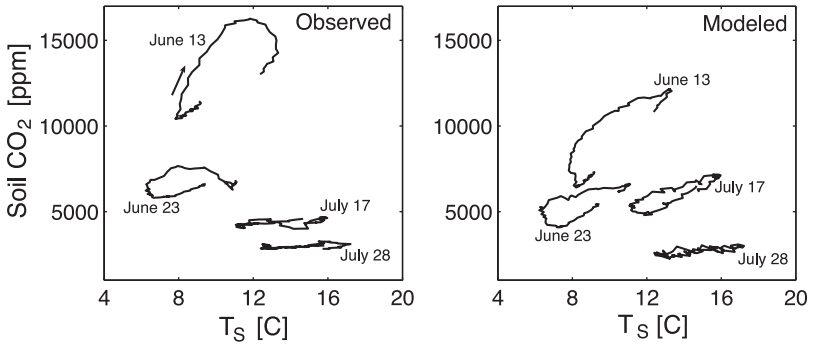

Figure 5. Observed and simulated diel variation of soil [CO_2] at 20 cm of the riparian site. Clockwise hysteresis (as indicated by the arrow) was observed in all measured and modeled [CO_2].

more sensitive to γ_H and h_b than to any other individual parameter as indicated by a steeper gradient in the highest model efficiencies. Figure 2 additionally indicates that there is asymmetry in the distribution of the sensitivity, depending on whether soil moisture is increasing or decreasing. The parameter h_b shows some degree of threshold behavior whereby model simulations appear highly sensitive to values of h_b below 50 cm, even though higher values are still feasible. While these plots do not include parameter interactions, they help inform which model parameters best constrain overall model uncertainty. Microbial communities have been found to be quite heterogeneous in space [*Fierer et al.*, 2003] and time [*Lipson and Schmidt*, 2004] as a function of soil temperature [*Zogg et al.*, 1997] and soil moisture [*Kieft et al.*, 1993; *Lundquist et al.*, 1999; *Schimel et al.*, 1999]. In addition, *Fierer and Jackson* [2006] demonstrated that soil pH was correlated to the diversity of soil microbial communities at large scales. We measured vadose zone soil water pH from a subset of lower hillslope and riparian landscape positions and did not observe strong variability (pH ~7.5; unpublished data). Nonetheless, soil pH could be an important variable and in some locations should be considered when modeling biogeochemical processes at the catchment scale. Additional ways to parametrize the variability of microbial activity, the lateral mobilization of soil organic matter and litter, and the effects of small precipitation events, will also be needed as catchment scale biogeochemical models are further developed.

[27] Modeling the subsurface as a single layer is a simplification of reality, but by doing so we could evaluate effects of patterns of seasonal soil moisture on biogeochemical processes across the entire watershed (Figure 9). We acknowledge that a multilayer model may yield different and certainly more detailed results across individual soil profiles; however, a single-layer model was useful to examine the effects of laterally variable environmental gradients on catchment scale soil CO_2 efflux. TOPMODEL is commonly configured with a single subsurface layer [e.g., *Scanlon et al.*, 2005] that still facilitates vertical and lateral soil moisture dynamics while it avoids additional uncertainties and potential equifinality associated with multiple soil layers. The result is that while the soil vertical structure is simplified, the model simulates the observations of soil CO_2 efflux across a large portion of the landscape. Our results suggest that the model has the ability to reproduce soil CO_2 generating processes (autotrophic and heterotrophic) in addition to diffusion-related feedbacks at diel time scales. These are important improvements from traditional power-based models [*Lloyd and Taylor*, 1994] or empirical relationships that are applied uniformly across the catchment [e.g., *Riveros-Iregui and McGlynn*, 2009].

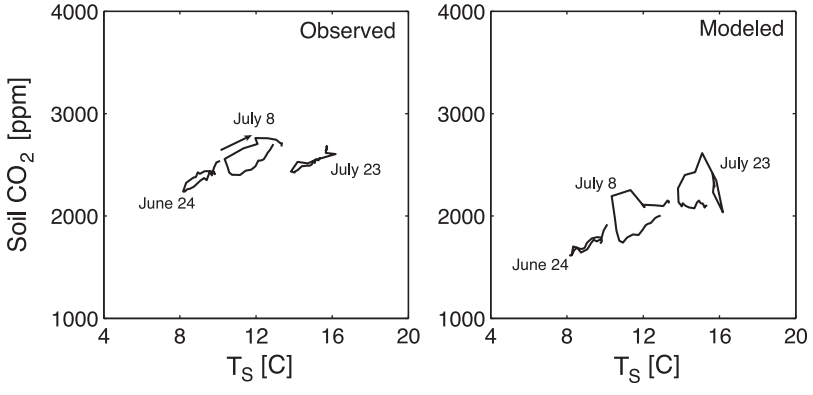

Figure 6. Observed and simulated diel variation of soil [CO_2] at 20 cm of the upland site. Clockwise hysteresis (as indicated by the arrow) was observed in all measured and modeled [CO_2]. Note the different scale in the *y* axis compared to Figure 5.

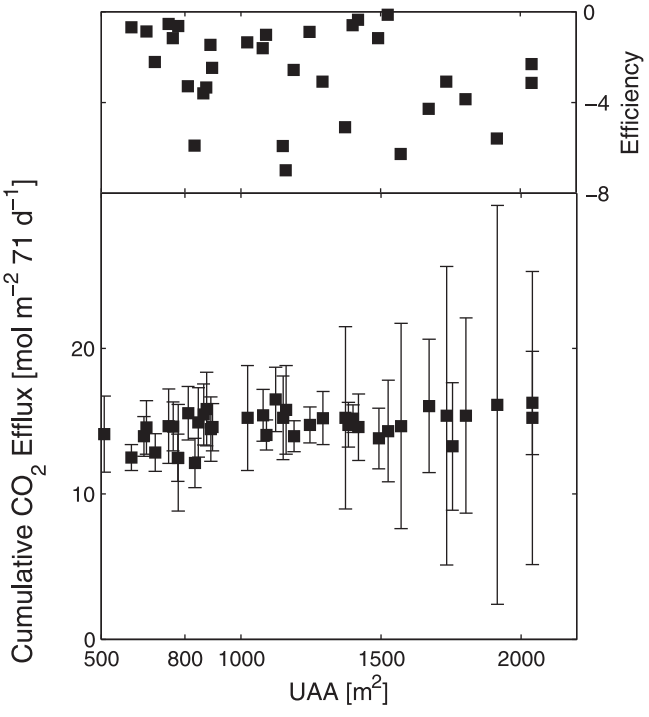

Figure 7. (top) Model efficiency (E) estimated at upland sites and compared with independent measurements reported by *Riveros-Iregui and McGlynn* [2009]. (bottom) Estimated cumulative soil CO_2 efflux (boxes) at the same sites for the 2006 growing season. Error bars indicate mean absolute error (MAE) compared to measured soil CO_2 efflux for the same period at each site. Model performance was better in areas with low UAA (i.e., dry, upland forests).

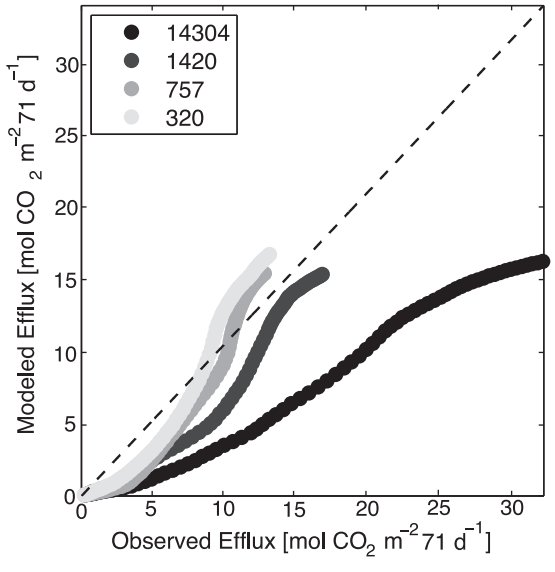

Figure 8. Observed versus modeled seasonal (cumulative) soil CO_2 efflux (mol CO_2 m^{-2}) over a 71 day period at four sites with variable upslope accumulated area (UAA). UAA (m^2) for each site is notated by color intensity where darker tones represent larger UAA.

[28] A current issue in modeling biogeochemical processes at the watershed scale is validation against independent observations. Many models that do not appear to suffer from limitations lack assessment against observations that represent the system for which the model is intended (although see *Richardson et al.* [2006] for a study where such assessments have been made). Assessment for the entire catchment revealed that modeled efflux was on average 11.1 mol CO_2 m^{-2} 71 $days^{-1}$, which were below empirically modeled catchment efflux (15.3 mol CO_2 m^{-2} 71 $days^{-1}$ [*Riveros-Iregui and McGlynn*, 2009]), but comparable to nighttime ecosystem respiration from an eddy covariance system installed over the forest (11.9 mol CO_2 m^{-2} over the same period [*Riveros-Iregui et al.*, 2008]). However, assessment selecting only sites with large drainage area (e.g., riparian meadows) indicated that the agreement between observed versus modeled efflux was considerably lower at these sites (i.e., observed efflux was almost twice as high as modeled efflux; Figure 8). As demonstrated in previous studies for this catchment [*Jencso et al.*, 2009; *Riveros-Iregui and McGlynn*, 2009], riparian meadows account for 2% of total catchment area, thus model performance at these sites has low impact on overall catchment flux. The spatial patterns in catchment efflux at different times of the year (Figure 9) confirmed field observations of differential timing for peaks in CO_2 production and CO_2 diffusion, and are in agreement with the hypothesis of spatially variable optimality of efflux [*Pacific et al.*, 2008, 2009, 2011]. Taken together, these results show that our modeling approach simulates lateral differences in CO_2 production and CO_2 diffusion across different times of the year, and it is a much more realistic approach than lumped models at the catchment scale that cannot simulate this fundamental, distributed behavior of heterogeneous landscapes.

[29] Our study demonstrates that the synergistic nature of full model-data integration can provide bidirectional feedback, as process models benefit from field knowledge, and new empirical data, new field observations, and new field experiments can be further designed and expanded based upon modeling results. We as a community are at a stage in which field observations are becoming increasingly available; thus generating models that realistically simulate the coupling of hydrological and biogeochemical processes, and at the same time make use of spatiotemporal data, is a way to move watershed science forward. It is anticipated that the spatiotemporal interdependencies of variables will remain difficult to measure, synthesize into conceptual frameworks, represent mathematically, and parametrize. Even with adequate conceptualization and model structure, watershed process parametrization will be problematic. This study provides important insight into coupling hydrological and biogeochemical models at landscape scales, and highlights the role of landscape structure and heterogeneity when modeling spatial variability of biogeochemical processes.

6. Conclusions

[30] We modified and applied an existing process soil CO_2 production and efflux model to a well-studied, topographically complex watershed of the northern Rocky Mountains. The model performed well in three areas. (1) It simulated the seasonality of soil [CO_2] at a riparian site,

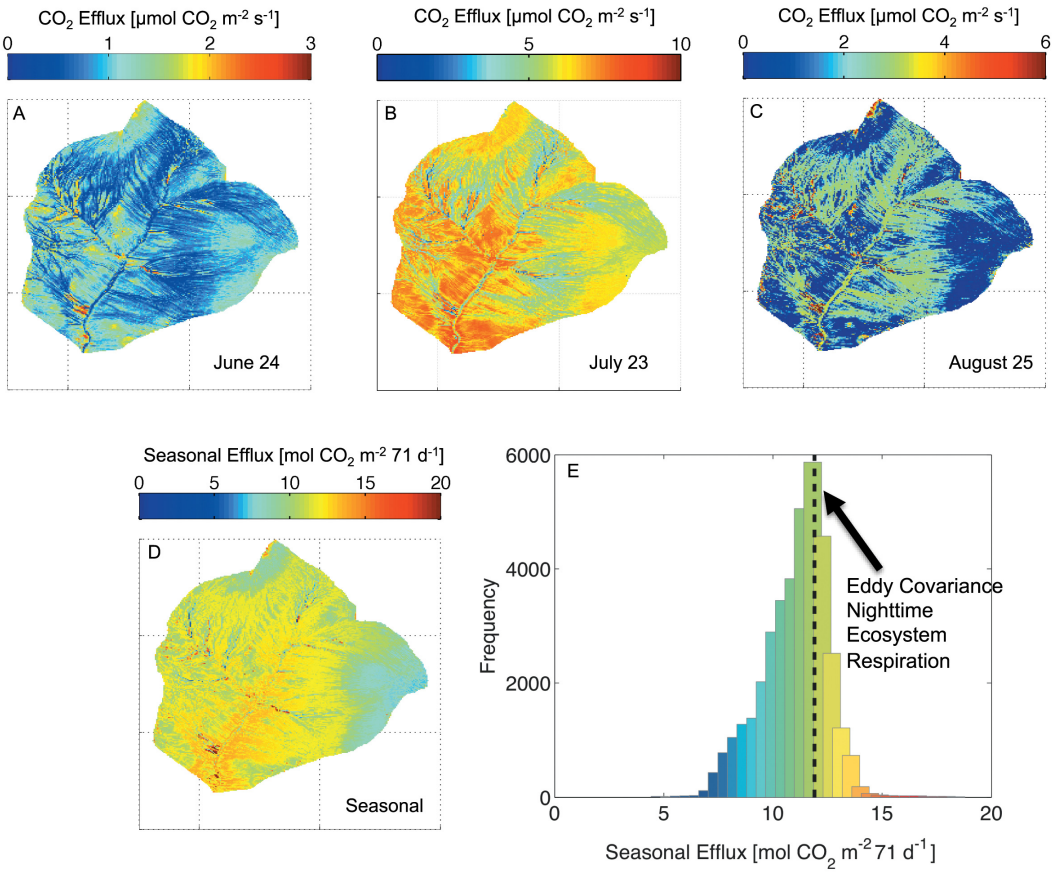

Figure 9. Spatiotemporal patterns of modeled soil CO_2 efflux across the 393 ha Stringer Creek watershed. (a–c) Snapshot in time during early, peak, and late growing season, made at 1400 LT on the indicated day. (d) Seasonal (cumulative) soil CO_2 efflux over 71 days. (e) Distribution of cells in d relative to eddy covariance nighttime ecosystem respiration reported by *Riveros-Iregui et al.* [2008]. Note that colorbars have different scales and units to enhance catchment differences. See Figure 1 for catchment UTM coordinates.

especially after implementation of a diffusion-limited component; (2) it reproduced short-term (diel) dynamics of soil $[CO_2]$, particularly hysteresis patterns in the soil $[CO_2]$–soil temperature relationship; and (3) it simulated seasonal estimates of soil CO_2 efflux at dry sites of the landscape. The model performed poorly when simulating seasonal (cumulative) soil CO_2 efflux at sites with large drainage area, likely as a result of poorly modeled soil water content at these sites and poorly parametrized microbial activity. We suggest that future watershed-scale biogeochemical models focus on improving spatial characterization of soil moisture and root and microbial respiration rates. Enhanced parametrization of the variability of these factors will improve our understanding of biogeochemical processes governing land-atmosphere exchange of CO_2.

[31] This study clearly demonstrated that if only modeled estimates of seasonal estimates of soil CO_2 efflux at dry sites were taken into account, these estimates would compare well with independent estimates of measured soil CO_2 efflux and independent eddy-covariance estimates of nighttime ecosystem respiration. However, our results also unveiled potential deficiencies when existing biogeochemical models are applied across strong soil moisture gradients in the landscape, and highlight the role of model assessment, experimental design, and the need for new observations that couple hydrological and biogeochemical understanding at the watershed scale, particularly in areas of pronounced topography.

[32] **Acknowledgments.** Financial support was provided by the U.S. National Science Foundation Integrated Carbon Cycle Research Program (EAR-0404130, EAR-0403924, EAR-0403906), and the Hydrologic Sciences Program (EAR-0337650, EAR-0837937, EAR-0838193, EAR-0943640). D.A. Riveros-Iregui acknowledges support from the 2007 American Geophysical Union Horton Research grant, a NSF Doctoral Dissertation Improvement grant (DEB-0807272), and the USGS 104b grant Program, administered by the MT Water Center. Airborne Laser Mapping was provided by the NSF-supported National Center for Airborne Laser Mapping (NCALM) at the University of CA, Berkeley. We thank Ward McCaughey of the USDA, Forest Service Rocky Mountain Research Station and the Tenderfoot Creek Experimental Forest for site access and logistical support. We are thankful for field assistance from Vince Pacific, Becca McNamara, Kelley Conde, and Austin Allen, GIS assistance from Kelsey Jencso and Rob Payn, and modeling discussions from Andres Munoz and Roberto Hincapie. Three anonymous reviewers and the associate editor provided valuable suggestions for the improvement of this manuscript.

References

Baldocchi, D., J. W. Tang, and L. K. Xu (2006), How switches and lags in biophysical regulators affect spatial-temporal variation of soil respiration in an oak-grass savanna, *J. Geophys. Res.*, *111*, G02008, doi:10.1029/2005JG000063.

Beven, K. J., and M. J. Kirkby (1979), A physically based, variable contributing area model of basin hydrology., *Hydrol. Sci. Bull.*, *24*(1), 43–69.

Campbell, E. P., D. R. Fox, and B. C. Bates (1999), A Bayesian approach to parameter estimation and pooling in nonlinear flood event models, *Water Resour. Res.*, *35*(1), 211–220, doi:10.1029/1998WR900043.

Campbell, G. S. (1974), A simple method for determining unsaturated conductivity from moisture retention data, *Soil Sci.*, *117*, 311–314.

Clapp, R. B., and G. M. Hornberger (1978), Empirical equations for some soil hydraulic properties, *Water Resour. Res.*, *14*, 601–604, doi:10.1029/WR014i004p00601.

Davidson, E. A., L. V. Verchot, J. H. Cattanio, I. L. Ackerman, and J. E. M. Carvalho (2000), Effects of soil water content on soil respiration in forests and cattle pastures of eastern Amazonia, *Biogeochemistry*, *48*(1), 53–69.

Emanuel, R. E., H. E. Epstein, B. L. McGlynn, D. L. Welsch, D. J. Muth, and P. D'Odorico (2010), Spatial and temporal controls on watershed ecohydrology in the northern Rocky Mountains, *Water Resour. Res.*, *46*, W11553, doi:10.1029/2009WR008890.

Fang, C., and J. B. Moncrieff (1999), A model for soil CO_2 production and transport. 1: Model development, *Agric. For. Meteorol.*, *95*(4), 225–236.

Farnes, P. E., R. C. Shearer, W. W. McCaughey, and K. J. Hansen (1995), Comparisons of Hydrology, Geology, and Physical Characteristics Between Tenderfoot Creek Experimental Forest (East Side) Montana, and Coram Experimental Forest (West Side) Montana. Final Report RJVA-INT-92734. USDA Forest Service, Intermountain Research Station, Forestry Sciences Laboratory. Bozeman, MT. *Rep.*, 19 pp.

Fierer, N., and R. B. Jackson (2006), The diversity and biogeography of soil bacterial communities, *Proc. Nat. Acad. Sci. U.S.A.*, *103*(3), 626–631.

Fierer, N., J. P. Schimel, and P. A. Holden (2003), Variations in microbial community composition through two soil depth profiles, *Soil Biol. Biochem.*, *35*(1), 167–176.

Freer, J., K. Beven, and B. Ambroise (1996), Bayesian estimation of uncertainty in runoff prediction and the value of data: An application of the GLUE approach, *Water Resour. Res.*, *32*(7), 2161–2173, doi:10.1029/95WR03723.

Grayson, R., and A. Western (2001), Terrain and the distribution of soil moisture, *Hydrol. Process.*, *15*(3), 2689–2690.

Hamman, S. T., I. C. Burke, and E. E. Knapp (2008), Soil nutrients and microbial activity after early and late season prescribed burns in a Sierra Nevada mixed conifer forest, *For. Ecol. Manage.*, *256*(3), 367–374.

Janssens, I. A., et al. (2001), Productivity overshadows temperature in determining soil and ecosystem respiration across European forests, *Global Change Biol.*, *7*(3), 269–278.

Jencso, K. G., B. L. McGlynn, M. N. Gooseff, S. M. Wondzell, K. E. Bencala, and L. A. Marshall (2009), Hydrologic connectivity between landscapes and streams: Transferring reach and plot scale understanding to the catchment scale, *Water Resour. Res.*, *45*, W04428, doi:10.1029/2008WR007225.

Jolly, W. M., J. M. Graham, A. Michaelis, R. Nemani, and S. W. Running (2005), A flexible, integrated system for generating meteorological surfaces derived from point sources across multiple geographic scales, *Environ. Model. Software*, *20*(7), 873–882.

Kane, E. S., D. W. Valentine, G. J. Michaelson, J. D. Fox, and C.-L. Ping (2006), Controls over pathways of carbon efflux from soils along climate and black spruce productivity gradients in interior Alaska, *Soil Biol. Biochem.*, *28*, 1438–1450.

Kang, S., S. Kim, S. Oh, and D. Lee (2000), Predicting spatial and temporal patterns of soil temperature based on topography, surface cover and air temperature, *For. Ecol. Manage.*, *136*(1–3), 173–184.

Kawamoto, K., P. Moldrup, P. Schjonning, B. V. Iversen, D. E. Rolston, and T. Komatsu (2006), Gas transport parameters in the vadose zone: Gas diffusivity in field and lysimeter soil profiles, *Vadose Zone J.*, *5*(4), 1194–1204.

Kieft, T. L., P. S. Amy, F. J. Brockman, J. K. Fredrickson, B. N. Bjornstad, and L. L. Rosacker (1993), Microbial abundance and activities in relation to water potential in the vadose zones of arid and semiarid sites, *Microbiol. Ecol.*, *26*(1), 59–78.

Knohl, A., A. R. B. Soe, W. L. Kutsch, M. Gockede, and N. Buchmann (2008), Representative estimates of soil and ecosystem respiration in an old beech forest, *Plant Soil*, *302*(1–2), 189–202.

Kucera, C. L., and D. R. Kirkham (1971), Soil respiration studies in tallgrass prairie in Missouri, *Ecology*, *52*(5), 912.

Lee, H., E. A. G. Schuur, J. G. Vogel, M. Lavoie, D. Bhadra, and C. L. Staudhammer (2011), A spatially explicit analysis to extrapolate carbon fluxes in alpine tundra where permafrost if thawing, *Global Change Biol.*, *17*, 1379–1393, doi:10.1111/j.1365-2486.2010.02287.x.

Lipson, D. A., and S. K. Schmidt (2004), Seasonal changes in an alpine soil bacterial community in the Colorado Rocky Mountains, *Appl. Environ. Microbiol.*, *70*(5), 2867–2879.

Liu, Q., N. T. Edwards, W. M. Post, L. Gu, J. Ledford, and S. Lenhart (2006), Temperature-independent diel variation in soil respiration observed from a temperate deciduous forest, *Global Change Biol.*, *12*(1), 2136–2145.

Liu, X. Z., S. Q. Wan, B. Su, D. F. Hui, and Y. Q. Luo (2002), Response of soil CO_2 efflux to water manipulation in a tallgrass prairie ecosystem, *Plant Soil*, *240*(2), 213–223.

Lloyd, J., and J. A. Taylor (1994), On the temperature-dependence of soil respiration, *Funct. Ecol.*, *8*(3), 315–323.

Lundquist, E. J., K. M. Scow, L. E. Jackson, S. L. Uesugi, and C. R. Johnson (1999), Rapid response of soil microbial communities from conventional, low input, and organic farming systems to a wet/dry cycle, *Soil Biol. Biochem.*, *31*(2), 1661–1675.

McGlynn, B. L., and J. Seibert (2003), Distributed assessment of contributing area and riparian buffering along stream networks, *Water Resour. Res.*, *39*(4), 1090, doi:10.1029/2002WR001525.

Moldrup, P., T. Olesen, T. Yamaguchi, P. Schjonning, and D. E. Rolston (1999), Modeling diffusion and reaction in soils: IX. The Buckingham-Burdine-Campbell equation for gas diffusivity in undisturbed soil, *Soil Sci.*, *164*(8), 542–551.

Moldrup, P., T. Olesen, S. Yoshikawa, T. Komatsu, and D. E. Rolston (2005a), Predictive-descriptive models for gas and solute diffusion coefficients in variably saturated porous media coupled to pore-size distribution: I. Gas dlifusivity in repacked soil, *Soil Sci.*, *170*(1), 843–853.

Moldrup, P., T. R. Olesen, S. Yoshikawa, T. Komatsu, and D. E. Rolston (2005b), Predictive-descriptive models for gas and solute diffusion coefficients in variably saturated porous media coupled to pore-size distribution: II. Gas diffusivity in undisturbed soil, *Soil Sci.*, *170*(1), 854–866.

Moncrieff, J. B., and C. Fang (1999), A model for soil CO_2 production and transport. 2: Application to a Florida Pinus elliotte plantation, *Agric. For. Meteorol.*, *95*(4), 237–256.

Nash, J. E., and J. V. Sutcliffe (1970), River flow forecasting through conceptual models. I. A discussion of principles, *J. Hydrol.*, *10*, 282–290.

Olesen, T., P. Moldrup, K. Henriksen, and L. W. Petersen (1996), Modeling diffusion and reaction in soils. 4. New models for predicting ion diffusivity, *Soil Sci.*, *161*(10), 633–645.

Orchard, V. A., and F. J. Cook (1983), Relationship between soil respiration and soil-moisture, *Soil Biol. Biochem.*, *15*(4), 447–453.

Pacific, V. J., B. L. McGlynn, D. A. Riveros-Iregui, D. L. Welsch, and H. E. Epstein (2008), Variability in soil respiration across riparian-hillslope transitions, *Biogeochemistry*, *91*, 51–70, doi:10.1007/s10533-008-9258-8.

Pacific, V. J., B. L. McGlynn, D. A. Riveros-Iregui, H. E. Epstein, and D. L. Welsch (2009), Differential soil respiration responses to changing hydrologic regimes, *Water Resour. Res.*, *45*, W07201, doi:10.1029/2009WR007721.

Pacific, V. J., B. L. McGlynn, D. A. Riveros-Iregui, D. L. Welsch, and H. E. Epstein (2011), Landscape structure, groundwater dynamics, and soil water content influence soil respiration across riparian-hillslope transitions, Tenderfoot Creek Experimental Forest, Montana., *Hydrol. Process.*, *25*, 811–827, doi:10.1002/hyp.7870.

Parton, W. J., D. S. Schimel, C. V. Cole, and D. S. Ojima (1987), Analysis of factors controlling soil organic-matter levels in Great-Plains grasslands, *Soil Sci. Soc. Am. J.*, *51*(5), 1173–1179.

Potter, C. S., J. T. Randerson, C. B. Field, P. A. Matson, P. M. Vitousek, H. A. Mooney, and S. A. Klooster (1993), Terrestrial ecosystem production - A process model-based on global satellite and surface data, *Global Biogeochem. Cycles*, *7*(4), 811–841.

Raich, J. W., and K. J. Nadelhoffer (1989), Belowground carbon allocation in forest ecosystems—Global trends, *Ecology*, *70*(5), 1346–1354.

Rastetter, E. B., M. G. Ryan, G. R. Shaver, J. M. Melillo, K. J. Nadelhoffer, J. E. Hobbie, and J. D. Aber (1991), A general biogeochemical model describing the responses of the C-cycle and N-cycle in terrestrial ecosystems to changes in CO_2, climate, and N-deposition, *Tree Physiol.*, *9*(1–2), 101–126.

Rastetter, E. B., G. I. Agren, and G. R. Shaver (1997), Responses of N-limited ecosystems to increased CO_2: A balanced-nutrition, coupled-element-cycles model, *Ecol. Appl.*, *7*(2), 444–460.

Ratkowsky, D. A., J. Olley, T. A. McMeekin, and A. Ball (1982), Relationship between temperature and growth-rate of bacterial cultures, *J. Bacteriol.*, *149*(1), 1–5.

Raupach, M. R., and J. J. Finnigan (1988), Single-layer models of evaporation from plant canopies are incorrect but useful, whereas multilayer models are correct but useless, *Aust. J. Plant Physiol.*, *15*, 705–716.

Reichstein, M., et al. (2003), Modeling temporal and large-scale spatial variability of soil respiration from soil water availability, temperature and vegetation productivity indices, *Global Biogeochem. Cycles*, *17*(4), 1104, doi:10.1029/2003GB002035.

Resurreccion, A. C., K. Kawamoto, T. Komatsu, P. Moldrup, K. Sato, and D. E. Rolston (2007), Gas diffusivity and air permeability in a volcanic ash soil profile: Effects of organic matter and water retention, *Soil Sci.*, *172*(6), 432–443.

Ricciuto, D. M., M. P. Butler, K. J. Davis, B. D. Cook, P. S. Bakwin, A. Andrews, and R. M. Teclaw (2008), Causes of interannual variability in ecosystem-atmosphere CO_2 exchange in a northern Wisconsin forest using a Bayesian model calibration, *Agric. For. Meteorol.*, *148*(2), 309–327.

Richardson, A. D., et al. (2006), Comparing simple respiration models for eddy flux and dynamic chamber data, *Agric. For. Meteorol.*, *141*(2–4), 219–234.

Riveros-Iregui, D. A., and B. L. McGlynn (2009), Landscape structure control on soil CO_2 efflux variability in complex terrain: Scaling from point observations to watershed scale fluxes, *J. Geophys. Res.*, *114*, G02010, doi:10.1029/2008JG000885.

Riveros-Iregui, D. A., R. E. Emanuel, D. J. Muth, B. L. McGlynn, H. E. Epstein, D. L. Welsch, V. J. Pacific, and J. M. Wraith (2007), Diurnal hysteresis between soil CO_2 and soil temperature is controlled by soil water content, *Geophys. Res. Lett.*, *34*, L17404, doi:10.1029/2007GL030938.

Riveros-Iregui, D. A., B. L. McGlynn, H. E. Epstein, and D. L. Welsch (2008), Interpretation and evaluation of combined measurement techniques for soil CO_2 efflux: Discrete surface chambers and continuous soil CO_2 concentration probes, *J. Geophys. Res.*, *113*, G04027, doi:10.1029/2008JG000811.

Rolston, D. E., and P. Moldrup (2002), Gas diffusivity, in *Methods of Soil Analysis – Part 4: Physical Methods*, edited by J. H. Dane and G. C. Topp, pp. 1113–1139, Soil Science Society of America, Madison, WI.

Ryan, M. G., R. M. Hubbard, S. Pongracic, R. J. Raison, and R. E. McMurtrie (1996), Foliage, fine-root, woody-tissue and stand respiration in Pinus radiata in relation to nitrogen status, *Tree Physiol.*, *16*(3), 333–343.

Saiz, G., K. Black, B. Reidy, S. Lopez, and E. P. Farrell (2007), Assessment of soil CO_2 efflux and its components using a process-based model in a young temperate forest site, *Geoderma*, *139*(1–2), 79–89.

Scanlon, T. M., G. Kiely, and R. Amboldi (2005), Model determination of non-point source phosphorus transport pathways in a fertilized grassland catchment, *Hydrol. Process.*, *19*(4), 2801–2814.

Schimel, J. P., J. M. Gulledge, J. S. Clein-Curley, J. E. Lindstrom, and J. F. Braddock (1999), Moisture effects on microbial activity and community structure in decomposing birch litter in the Alaskan taiga, *Soil Biol. Biochem.*, *31*(6), 831–838.

Seibert, J., and B. L. McGlynn (2007), A new triangular multiple flow direction algorithm for computing upslope areas from gridded digital elevation models, *Water Resour. Res.*, *43*(4), W04501, doi:10.1029/2006WR005128.

Simunek, J., and D. L. Suarez (1993), Modeling of carbon-dioxide transport and production in soil. 1. Model development, *Water Resour. Res.*, *29*(2), 487–497, doi:10.1029/92WR02225.

Suarez, D. L., and J. Simunek (1993), Modeling of carbon-dioxide transport and production in soil. 2. Parameter selection, sensitivity analysis, and comparison of model predictions to field data, *Water Resour. Res.*, *29*(2), 499–513, doi:10.1029/92WR02226.

Tang, J. W., L. Misson, A. Gershenson, W. X. Cheng, and A. H. Goldstein (2005), Continuous measurements of soil respiration with and without roots in a ponderosa pine plantation in the Sierra Nevada Mountains, *Agric. For. Meteorol.*, *132*(3–4), 212–227.

van Genuchten, M. T. (1980), A closed-form equation for predicting the hydraulic conductivity of unsaturated soils, *Soil Sci. Soc. Am. J.*, *44*(5), 892–898.

Vargas, R., and M. F. Allen (2008), Environmental controls and the influence of vegetation type, fine roots and rhizomorphs on diel and seasonal variation in soil respiration, *New Phytologist*, *179*(2), 460–471.

Wagener, T. (2003), Evaluation of catchment models, *Hydrol. Process.*, *17*(6), 3375–3378.

Welsch, D. L., and G. M. Hornberger (2004), Spatial and temporal simulation of soil CO_2 concentrations in a small forested catchment in Virginia, *Biogeochemistry*, *71*(3), 415–436.

Western, A. W., and R. B. Grayson (1998), The Tarrawarra data set: Soil moisture patterns, soil characteristics, and hydrological flux measurements, *Water Resour. Res.*, *34*(10), 2765–2768, doi:10.1029/98WR01833.

Winkler, J. P., R. S. Cherry, and W. H. Schlesinger (1996), The Q(10) relationship of microbial respiration in a temperate forest soil, *Soil Biol. Biochem.*, *28*(8), 1067–1072.

Woods, S. W., R. Ahl, J. Sappington, and W. McCaughey (2006), Snow accumulation in thinned lodgepole pine stands, Montana, USA, *For. Ecol. Manage.*, *235*(1-3), 202–211.

Yuste, J. C., I. A. Janssens, A. Carrara, L. Meiresonne, and R. Ceulemans (2003), Interactive effects of temperature and precipitation on soil respiration in a temperate maritime pine forest, *Tree Physiol.*, *23*(8), 1263–1270.

Zogg, G. P., D. R. Zak, D. B. Ringelberg, N. W. MacDonald, K. S. Pregitzer, and D. C. White (1997), Compositional and functional shifts in microbial communities due to soil warming, *Soil Sci. Soc. Am. J.*, *61*(2), 475–481.

R. E. Emanuel, Department of Forestry and Environmental Resources, North Carolina State University, Raleigh, NC 27695, USA.

H. E. Epstein, Department of Environmental Sciences, University of Virginia, Charlottesville, VA 22904, USA.

L. A. Marshall and B. L. McGlynn, Department of Land Resources and Environmental Sciences, Montana State University, 334 Leon Johnson Hall, Bozeman, MT 59717, USA.

D. A. Riveros-Iregui, School of Natural Resources, University of Nebraska, 3310 Holdrege St., Lincoln, NE 68583-0995, USA. (driveros2@unl.edu)

D. L. Welsch, Canaan Valley Institute, Davis, WV 26260, USA.